Journal of Chemical Health Risks
www.jchr.org
JCHR (2025) 15(4), 1118-1124 | ISSN:2251-6727

FT-IR, SEM, XRD and Antimicrobial Effect of ZNO Nanoparticles Synthesised from Marine Plant Leaf (Rhizophora Apiculata)

S. Prabha

Department of Chemistry, Government Arts College, B. Mutlur, Chidambaram-608102, Tamilnadu, India

(Received: 16 May 2025 Revised: 20 June 2025 Accepted: 12 July 2025)

KEYWORDS

Zinc oxide nanoparticles, Green synthesis, Rhizophora apiculate, FT-IR, SEM, X-ray diffraction, Anti-microbial activity.

ABSTRACT:

In this study, zinc oxide (ZnO) nanoparticles were successfully synthesized via a green route . The extract was prepared by boiling powdered leaves in distilled water, followed by filtration. Biosynthesis of ZnO nanoparticles was achieved by reacting zinc nitrate with the extract under controlled heating, and the product was subsequently calcined at 400°C. Characterization by Fourier-transform infrared spectroscopy (FTIR) revealed the involvement of functional groups such as hydroxyl, amide, and phenolic moieties in the reduction and stabilization of ZnO nanoparticles. Scanning electron microscopy (SEM) confirmed the formation of predominantly hexagonal and cubic nanoparticles, with sizes ranging from 30 to 80 nm. X-ray diffraction (XRD) analysis validated the hexagonal wurtzite crystal structure with high crystallinity and phase purity. The biosynthetic mechanism is attributed to the reducing and capping actions of phytochemicals like flavonoids, terpenoids, and proteins present in the extract. This environmentally benign synthesis approach demonstrates the potential of R. apiculata as a bio-factory for stable, nanoscale ZnO particles, suitable for applications in biomedical, catalytic and environmental domains.

Introduction

Nanotechnology has revolutionized material science, offering novel approaches for the synthesis of nanostructured materials with wide-ranging applications in fields such as medicine, catalysis, and environmental remediation [1]. Among metal oxide nanoparticles, zinc oxide (ZnO) has garnered significant attention due to its exceptional physicochemical properties, including high surface area, wide bandgap (3.37 eV), and strong photocatalytic and antimicrobial activities [2,3]. Conventional chemical and physical methods of ZnO nanoparticle synthesis often involve hazardous chemicals, high energy consumption, and pose environmental risks [4]. Consequently, the pursuit of green and sustainable synthesis methods has become a research priority. Biological or green synthesis methods, particularly those using plant extracts, offer an eco-friendly alternative for nanoparticle production. These methods utilize phytochemicals such as flavonoids, terpenoids, phenolics, and proteins, which act as natural reducing and stabilizing agents [5,6]. This approach not only reduces the reliance on toxic chemicals but also enhances biocompatibility and functionality of the synthesized nanoparticles [7].

Mangroves are salt-tolerant coastal vegetation which are rich in diverse bioactive compounds due to their unique ecological niche. Rhizophora apiculata, a dominant mangrove species found in the Pichavaram mangrove forest of Tamil Nadu, India, has been traditionally used in folk medicine for its antibacterial, anti-inflammatory, and antiseptic properties [8]. Previous phytochemical analyses of R. apiculata have confirmed the presence of alkaloids, tannins, and phenolic compounds, indicating its potential for green nanomaterial synthesis [9]. In this study, we report the green synthesis of ZnO nanoparticles using an aqueous leaf extract of R. apiculata. The synthesized nanoparticles were characterized using Fourier-transform infrared spectroscopy (FTIR), scanning electron microscopy (SEM), and X-ray diffraction (XRD) to determine their morphology,

Journal of Chemical Health Risks
www.jchr.org
JCHR (2025) 15(4), 1118-1124 | ISSN:2251-6727

crystallinity, and functional groups involved in the synthesis. The results demonstrate that the phytochemicals in R. apiculata act effectively as both reducing and capping agents, yielding stable ZnO nanoparticles with a crystalline hexagonal wurtzite structure. This green synthesis strategy represents a sustainable and efficient route for producing ZnO nanoparticles with potential applications in biomedical and environmental technologies. Metal-based nanoparticles have been extensively investigated for a set of biomedical applications. According to the World Health Organization, in addition to their reduced size and selectivity for bacteria, metal-based nanoparticles have also proved to be effective against pathogens listed as a priority. In recent research, antimicrobial activities of various metal nanoprticles are studied and reported that they shown good microbial effect against various pathogenic systems.

1. Experimental

Zinc nitrate was obtained from Sigma-Aldrich (India), while solvents such as ethanol, methanol and other reagents were sourced from Merck (India) and used without further purification. The plant Rhizophora apiculata (vernacularly known as Surapunnai in Tamil) was collected from the Pichavaram mangrove forest situated in Bay of Bengal near to Chidambaram, Cuddalore District, Tamil Nadu, which is the second-largest mangrove forest globally. The plant was authenticated at the herbarium of the Centre of Advanced Study (C.A.S.) in Marine Biology, Annamalai University, Parangipettai. Fresh leaves were washed, shade-dried, coarsely powdered and stored in airtight containers for further use. Morphological characteristics of R. apiculata include dark green leathery leaves, cream-coloured flowers and pear-shaped fruits. Medicinally, its extracts have been reported to possess antibacterial, anti-inflammatory and antiseptic properties.

2.1 Preparation of Plant Extract and Synthesis of ZnO Nanoparticles:

As shown in **Scheme-1**, about 50 g of powdered R. apiculata leaves were boiled with 100 mL of double-distilled water. After cooling, the solution was filtered through cotton cloth and Whatman No.1 filter paper, yielding a light green extract, which was refrigerated at 4°C for further use. For nanoparticle synthesis, 50 mL of this extract was heated to 60–80°C, and 5 g of zinc nitrate was gradually added as the temperature reached to 60°C. The mixture was continuously heated until it reduced to a pale-yellow paste, which was then transferred to a ceramic crucible and calcined in a furnace at 400°C for 2 hours [10]. The resulting light-yellow powder was ground to a fine consistency for characterization.

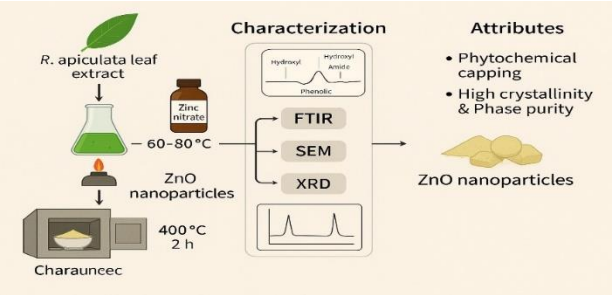

Scheme-1 Synthetic route of extract and its ZnO NPs

2. Results and discussion

2.1 FT-IR analysis

FTIR spectroscopy was employed to elucidate the functional groups responsible for the reduction and stabilization of ZnO nanoparticles synthesized using Rhizophora apiculata leaf extract. The spectral profiles of the raw extract are shown in **Figure 1** and the ZnO nanoparticles (**Figure 2**) revealed key differences indicative of biomolecular involvement in the biosynthesis process. In the spectrum of the R. apiculata leaf extract (Fig.1), a broad and intense peak centered at 3325.828 cm^{-1} and 3295.537 cm^{-1} corresponds to the O–H stretching vibrations of phenolic compounds and hydroxyl groups. These functional groups are widely reported to act as reducing agents in green nanoparticle synthesis [4]. A sharp peak at 1635.178 cm^{-1} indicates the C=O stretching of amide I bands, typically originating from proteins or polyphenols, which can also act as capping agents [11]. Other prominent absorption peaks include bands at 1369.478 cm^{-1}, which may be attributed to N–H bending of amines or O–H deformation, and 1219.615 cm^{-1}, likely due to C–O stretching in alcohols or esters. Minor peaks at 3737.835 cm^{-1}, 2545.978 cm^{-1} and in the 2100–2200 cm^{-1} region could relate to atmospheric CO_2 or weak alkyne/alkene overtones. In contrast, the FTIR spectrum of the ZnO nanoparticles (**Figure 2**) exhibits several noticeable spectral shifts and new peak formations, indicative of successful metal ion reduction and nanoparticle formation. The broad band near 3525.986 cm^{-1} and

Journal of Chemical Health Risks
www.jchr.org
JCHR (2025) 15(4), 1118-1124 | ISSN:2251-6727

3333.131 cm^{-1} corresponds to O–H stretching vibrations of residual hydroxyl groups or bound water molecules on the nanoparticle surface, suggesting continued interaction with phytochemicals post-synthesis. Peaks at 1695.222 cm^{-1} and 1507.898 cm^{-1} are attributed to O–H bending and aromatic ring vibrations, possibly from polyphenolic compounds acting as capping agents [12].

A notable new band at 1306.942 cm^{-1} is associated with C=N stretching vibrations, likely arising from proteins or amino groups bound to the nanoparticle surface. Most crucially, the characteristic Zn–O stretching vibration appears at 661.574 cm^{-1}, confirming the successful synthesis of ZnO nanoparticles [13].

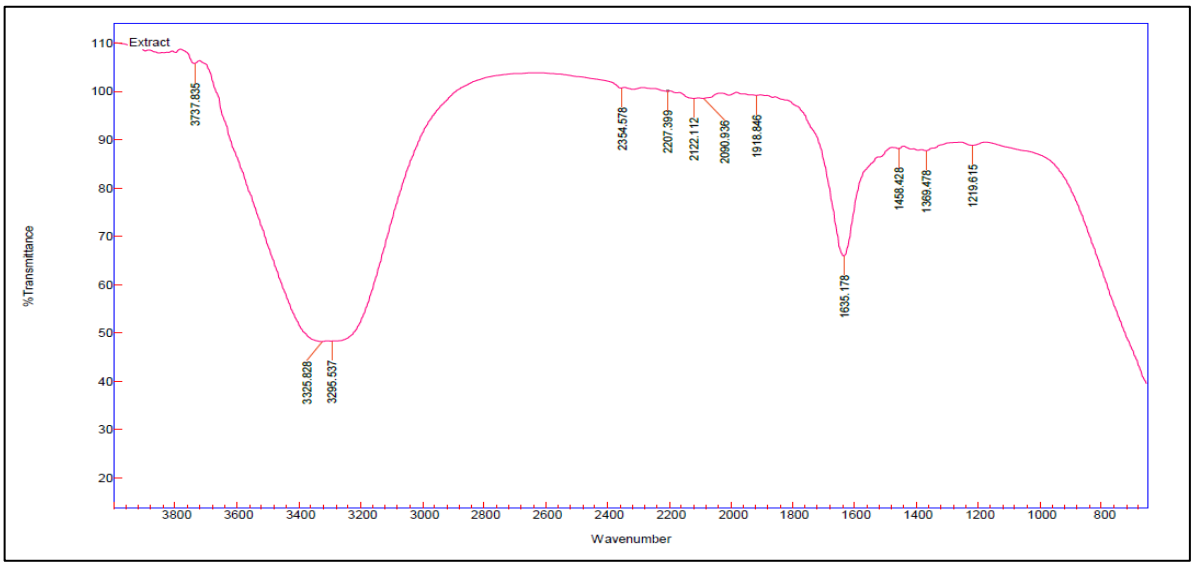

Figure 1 IR spectra of R.Apiculata leaf extract

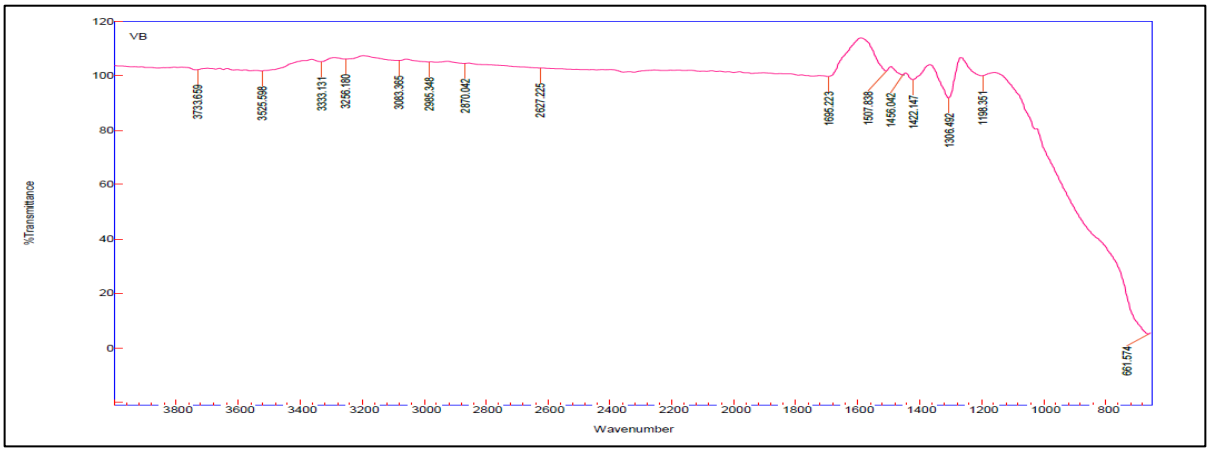

Figure 2 IR spectra of prepared ZnO nanoparicles using R.Apiculata leaf extract

Table-1 showed that several peaks originally present in the extract spectrum, such as those around 2545–2200 cm^{-1}, disappeared significantly in the nanoparticle spectrum, indicating their consumption or transformation during the synthesis process. Meanwhile, peaks such as 1452.044 cm^{-1}, 1422.412 cm^{-1} and 1198.395 cm^{-1} further support the presence of various phytochemicals involved in stabilization and surface functionalization.

Journal of Chemical Health Risks
www.jchr.org
JCHR (2025) 15(4), 1118-1124 | ISSN:2251-6727

Table-1 FT-IR frequencies of extract and ZnO-nanoparticle

Functional Group	Extract Peak (cm^{-1})	ZnO NPs Peak (cm^{-1})	Assignment
O–H Stretch	3325.828, 3295.537	3525.986, 3333.131	Hydroxyl/ Phenolics
C=O stretch of amide	1635.178	1695.222	Proteins/ Polyphenols
N–H/O–H bend	1369.478	1306.942	Amines/Proteins
C–O stretch of alcohols	1219.615	1198.395	Alcohols/Esters
Zn–O stretch	—	661.574	ZnO NPs confirmation

The comparative FTIR analysis clearly demonstrates the transformation of specific functional groups from the R. apiculata extract into the ZnO nanoparticle matrix. This supports the hypothesis that bioactive compounds such as phenolics, flavonoids, terpenoids, and proteins not only act as reducing agents but also play a critical role in nanoparticle capping and stabilization, thereby affirming the efficacy of green synthesis strategies.

3.2 SEM Analysis of ZnO Nanoparticles

Scanning Electron Microscopy (SEM) was used to examine the morphological features and surface topology of the ZnO nanoparticles synthesized using R. apiculata extract.

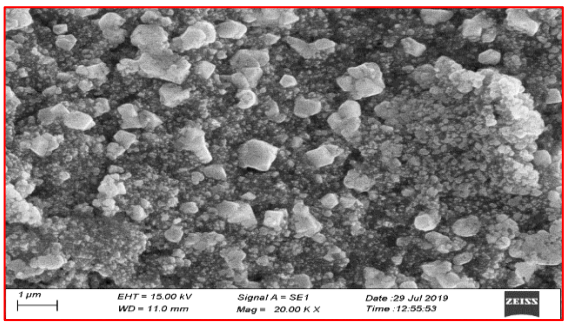

Figure 3. Scaning electron microscopy of ZnO nanoparticles using R. Apiculata leaf extract with scale bar 1µm at 20.00 K X magnification

Figure 3 shows that this micrograph reveals a relatively uniform distribution of particles with predominantly hexagonal and irregular spherical morphologies. The particles exhibit minimal aggregation and appear to be well dispersed, indicating effective capping by phytochemicals in the extract. The size range appears consistent, suggesting control over nucleation and growth during biosynthesis.

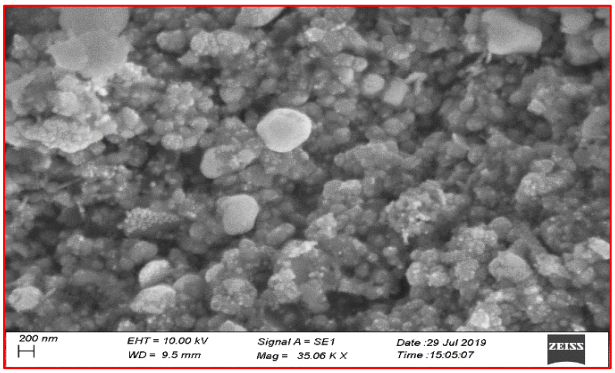

Figure 4 Scaning electron microscopy of ZnO nanoparticles using R. Apiculata leaf extract with scale bar 200nm at 35.06 K X magnification

At higher magnification (**Figure 4**), a more detailed view of particle surfaces and aggregation patterns is visible. The particles appear densely packed with distinguishable grain boundaries, and their average size ranges approximately from 30 to 80 nm, corroborating estimates derived from XRD analysis. The enhanced resolution reveals that smaller nanoparticles adhere around larger ones, possibly due to surface interactions or partial agglomeration. These SEM images demonstrate that the green synthesis using R. apiculata extract effectively produces nanocrystalline ZnO with controlled morphology and good dispersion, largely attributed to the presence of polyphenolic and proteinaceous compounds acting as capping agents [14, 15].

3.3 XRD Analysis of ZnO Nanoparticles Synthesized Using R. apiculata Leaf Extract

The crystalline structure of biosynthesized ZnO nanoparticles was investigated using X-ray diffraction (XRD) analysis, as shown in **Figure 5**. The XRD pattern

Journal of Chemical Health Risks
www.jchr.org
JCHR (2025) 15(4), 1118-1124 | ISSN:2251-6727

exhibits a series of well-defined peaks at 2θ values of approximately 31.7°, 34.4°, 36.2°, 47.5°, 56.6°, 62.8°, 66.4°, 67.9°, 69.1°, 72.6°, 77.0° and 79.2°, which correspond to the crystal planes (100), (002), (101), (102), (110), (103), (200), (112), (201), (004), and (202), respectively. These peaks are in excellent agreement with the standard diffraction data of hexagonal wurtzite ZnO (JCPDS card No. 36-1451) [16], confirming the formation of pure crystalline ZnO nanoparticles.

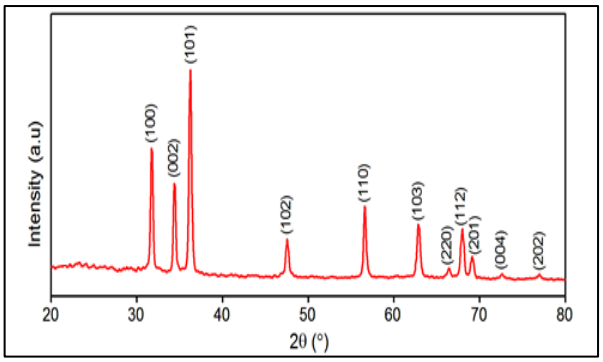

Figure 5. XRD Spectrum of Zinc oxide nanoparticles synthesized using R. apiculate plant leaf extract

The intense and narrow diffraction peaks reflect a high degree of crystallinity, while the absence of additional impurity peaks indicates that the synthesized ZnO nanoparticles are phase pure and free from any secondary or foreign phases. This strongly suggests that the R. apiculata extract plays a dual role as a reducing and stabilizing agent, facilitating the formation of nanocrystalline ZnO.

The average crystalline size (D) of the ZnO nanoparticles can be estimated using the Debye–Scherrer equation shown in equation (i).

$D=K\lambda/\beta\cos\theta$ …… (i)

where, K is the Scherrer constant,

λ is wave length of the X-ray beam used (1.54,184 Å),

β is the Full width at half maximum (FWHM) of the peak and

θ is the Bragg angle

Using the most intense peak at (101) plane, the calculated average crystallite size was found to be in the range of 20–40 nm, consistent with the morphology observed in SEM analysis. This nanoscale size can be attributed to the capping and growth-regulating effects of phytochemicals present in the R. apiculata extract, which control the nucleation and inhibit uncontrolled growth during synthesis [4, 15].

3.4 Proposed Mechanism of Biosynthesis

The biosynthesis mechanism of ZnO nanoparticles using R. apiculata leaf extract can be attributed to the synergistic activity of its bioactive constituents. Compounds such as flavonoids, terpenoids, phenolic acids, and proteins are involved in both the reduction of Zn^{2+} ions and stabilization of the resulting nanoparticles. Initially, zinc acetate precursors interact with functional groups, particularly hydroxyl and carbonyl moieties, which facilitate electron transfer and reduction. Post-reduction, proteins and polyphenols cap the growing nanoparticles, preventing their aggregation and promoting uniform nucleation. During calcination, the organic residues decompose, leaving behind stable, crystalline ZnO nanoparticles. This green synthesis process eliminates the need for toxic reducing agents, offering a sustainable alternative for nanoparticle production [17]. The presence of biomolecule residues even after synthesis, as evidenced by FTIR, indicates their enduring role in particle stabilization and functional performance, particularly in photocatalysis and antimicrobial applications.

3.5 Antimicrobial activity

Antibacterial and antifungal activities of present ZnO NPs are carriedout by using Kirby-Bauer disc diffusion method. The measured zone of inhibition values are shown in Table-2. Ampicillin is used as standard for antibacterial effect and Ciprofloxacin is used for antifungal effect. In both cases, the samples are dissolved in DMSO.

Table-2 Zone of inhibition(mm) values of antimicrobial activity of ZnO nanoparicles

Activity	Type of organism	Species	ZnO NPs (mm)	Std (mm)

Journal of Chemical Health Risks
www.jchr.org
JCHR (2025) 15(4), 1118-1124 | ISSN:2251-6727

Antibacterial activity	Gram positive Bacteria	*B.subtilis*	14	16
		M.luteus	15	16
		S.aureus	14	15
	Gram negative Bacteria	*E.coli*	16	16
		P.aeruginosa	12	14
Antifungal Activity	Fungal species	*A.niger*	10	10
		P.scup	9	10

ZnO NPs exhibited notable antibacterial activity against both Gram-positive and Gram-negative bacteria, with zones of inhibition measuring 14 mm for *Bacillus subtilis*, 15 mm for *Micrococcus luteus*, and 14 mm for *Staphylococcus aureus*, compared to standard antibiotics showing 15–16 mm inhibition. Among Gram-negative strains, *Escherichia coli* demonstrated the highest susceptibility (16 mm), followed by *Pseudomonas aeruginosa* (12 mm), which was slightly less responsive than the standard (14 mm). ZnO NPs also showed moderate antifungal activity, producing inhibition zones of 10 mm and 9 mm against *Aspergillus niger* and *Penicillium scup*, respectively, which closely matched those of the standard antifungal agents. These results are consistent with previous findings that attribute the antimicrobial activity of ZnO NPs to their ability to generate reactive oxygen species (ROS), disrupt microbial membranes, and release Zn^{2+} ions, leading to cellular damage and death [18-21]. The slight variations in sensitivity among the tested organisms highlight the influence of microbial cell wall structure and composition on ZnO NP efficacy [22, 23].

3. Conclusions

The study demonstrates the successful biosynthesis of ZnO nanoparticles using the aqueous leaf extract of Rhizophora apiculata. The FTIR spectra confirm the presence of organic functional groups acting as capping and stabilizing agents. SEM analysis reveals the formation of hexagonal and cubic nanoparticles with an average size ranging from 30–80 nm, while XRD confirms the hexagonal wurtzite structure with high crystallinity. This green approach leverages the biological activity of R. apiculata phytochemicals, promoting a sustainable and eco-friendly method for nanoparticle synthesis. The synthesized ZnO nanoparticles hold potential for diverse applications in biomedicine, catalysis, and environmental remediation. ZnO nanoparticles demonstrated significant antibacterial and moderate antifungal activity, comparable to standard antimicrobial agents. Their effectiveness is attributed to ROS generation, membrane disruption, and Zn^{2+} ion release, with variations depending on microbial cell structure.

Acknowledgments

Author thank the PG & Research Department of Chemistry, Govt. Arts College, Chidambaram for providing opportunity to carry out this research work.

References

1. Khan, I., Saeed, K. and Khan, I. (2019) Nanoparticles: Properties, applications and toxicities, *Arabian Journal of Chemistry*, 12(7), 908–931.
2. Zhang, L., Jiang, Y., Ding, Y., et al. (2007) Investigation into the antibacterial behaviour of suspensions of ZnO nanoparticles (ZnO nanofluids), *Journal of Nanoparticle Research*, 9, 479–489.
3. Sirelkhatim, A., Mahmud, S., Seeni, A., et al. (2015) Review on zinc oxide nanoparticles: Antibacterial activity and toxicity mechanism, *Nano-Micro Letters*, 7, 219–242.
4. Iravani, S. (2011) Green synthesis of metal nanoparticles using plants, *Green Chemistry*, 13(10), 2638–2650.
5. Singh, P., Kim, Y. J., Zhang, D. and Yang, D. C. (2016) Biological synthesis of nanoparticles

Journal of Chemical Health Risks
www.jchr.org
JCHR (2025) 15(4), 1118-1124 | ISSN:2251-6727

from plants and microorganisms, *Trends in Biotechnology*, 34(7), 588–599.

6. Barabadi, H., Vahidi, H., Kamali, K. D., et al. (2019) Emerging theranostic silver and gold nanomaterials to combat prostate cancer: A systematic review, *Journal of Cluster Science*, 30, 1375–1384.

7. Ahmed, S., Ahmad, M., Swami, B. L. and Ikram, S. (2016) A review on plant extract-mediated synthesis of silver nanoparticles for antimicrobial applications: A green expertise, *Journal of Advanced Research*, 7(1), 17–28.

8. Kathiresan, K. and Bingham, B. L. (2001) Biology of mangroves and mangrove ecosystems, *Advances in Marine Biology*, 40, 81–251.

9. Premanathan, M., Kathiresan, K., Yamamoto, N. and Nakashima, H. (1999) In vitro anti-human immunodeficiency virus activity of polysaccharide from *Rhizophora apiculata* bark, *Biological & Pharmaceutical Bulletin*, 22(11), 1071–1073.

10. Datta, A., Patra, C., Bharadwaj, H., Kaur, S., Dimri, N. and Khajuria, P. (2017) Green synthesis of zinc oxide nanoparticles using *Parthenium hysterophorus* leaf extract and evaluation of their antibacterial properties, *Journal of Biotechnology & Biomaterials*, 7(271), 1.

11. Sathishkumar, M., et al. (2009) *Cinnamomum zeylanicum* bark extract-mediated green synthesis of nano-crystalline silver particles, *Colloids and Surfaces B: Biointerfaces*, 73(2), 332–338.

12. Sundrarajan, M. and Gowri, S. (2011) Green synthesis of titanium dioxide nanoparticles by *Nyctanthes arbor-tristis* extract, *Chalcogenide Letters*, 8(8), 447–451.

13. Anil Kumar, H. S., Bhavi, S. M., Singh, S. R., Thokchom, B., Yarajarla, R. B. and Kotresha, D. (2025) Biosynthesis of silver nanoparticles using *Aristolochia bracteolata* Lam. ethyl acetate extract: Characterization and in vitro anticancer activity against lung adenocarcinoma cells, *Next Nanotechnology*, 7, 100174.

14. Alkaabi, Z. K. (2021) Synthesis and characterization of ZnO nanoparticles via *Aloe vera* extract, *Materials Science Forum*, 1039, 211–214.

15. Ramesh, P. S., Kokila, T. and Geetha, D. (2015) Plant-mediated green synthesis and antibacterial activity of silver nanoparticles using *Emblica officinalis* fruit extract, *Spectrochimica Acta Part A: Molecular and Biomolecular Spectroscopy*, 142, 339–343.

16. International Centre for Diffraction Data. (n.d.) *JCPDS File No. 36-1451*.

17. Kharissova, O. V., Dias, H. V. R., Kharisov, B. I., Pérez, B. O. and Pérez, V. M. (2013) The greener synthesis of nanoparticles, *Trends in Biotechnology*, 31(4), 240–248.

18. Raghupathi, K.R., Koodali, R.T., Manna, A.C. (2011). *Langmuir*, **27**, 4020–4028.

19. Sirelkhatim, A., Mahmud, S., Seeni, A., Kaus, N.H.M., Ann, L.C., Bakhori, S.K.M., Hasan, H., Mohamad, D. (2015). *Nano-Micro Lett.*, **7**, 219–242.

20. Padmavathy, N., Vijayaraghavan, R. (2008). *Sci. Technol. Adv. Mater.*, **9**, 035004. Premanathan, M., Karthikeyan, K., Jeyasubramanian, K., Manivannan, G. (2011). *Nanomedicine*, **7**, 184–188.

21. Zhang, L., Jiang, Y., Ding, Y., Daskalakis, N., Jeuken, L., Povey, M., O'Neill, A.J., York, D.W. (2007). *J. Nanopart. Res.*, **9**, 479–489.

22. Emami-Karvani, Z., Chehrazi, P. (2011). *J. Biol. Sci.*, **11**, 463–467.